1-30-2020

Improved Estimation for Saleh Model and Predistortion of Power Amplifiers using 1-dB Compression Point

Haider Al Kanan
Portland State University, haider2@pdx.edu

Xianzhen Yang
Portland State University, scottxzy@gmail.com

Fu Li
Portland State University, lif@pdx.edu

Citation Details

Al-kanan, H., Yang, X., & Li, F. (2020). Improved estimation for Saleh model and predistortion of power amplifiers using 1-dB compression point. The Journal of Engineering, 2020(1), 13-18.

The Journal of Engineering

Research Article

IET Journals
The Institution of Engineering and Technology

Improved estimation for Saleh model and predistortion of power amplifiers using 1-dB compression point

eISSN 2051-3305
Received on 28th June 2019
Revised 18th September 2019
Accepted on 27th September 2019
E-First on 11th December 2019
doi: 10.1049/joe.2019.0973
www.ietdl.org

Haider Al-kanan[1], Xianzhen Yang[1], Fu Li[1] ✉

[1]*Department of Electrical and Computer Engineering, Portland State University, OR 97207-0751, USA*
✉ *E-mail: lif@pdx.edu*

Abstract: This paper proposes an improved estimation approach for modelling RF power amplifiers (PAs) using the Saleh behavioural model. The proposed approach is appropriate for solid-state PA technologies. The 1-dB compression point of the PA is included in the estimation approach to improve the estimation of the Saleh coefficients. Thus, expressions are derived to describe the relationship between the parameters of the Saleh model and the manufacturing specifications of PAs: gain (G), third-order intercept point (IP_3) and 1-dB compression point (P_{1dB}). This method is a simple estimation of a memoryless amplitude-to-amplitude (AM/AM) nonlinearity to benefit RF designers evaluating the PA distortion using the PA parameters: P_{1dB}, G, and IP_3, before conducting experimental validation. The linearisation method using digital predistortion (DPD) is derived as a function of G, IP_3, and P_{1dB}, for mitigating the AM/AM nonlinear distortion. Finally, the modelling and DPD techniques are both evaluated using the experimental results of the GaAs PA.

1 Introduction

Behavioural modelling for power amplifiers (PAs) has become popular in modern wireless communications (i.e. 4G/5G wireless communications), as the PA circuit design and circuit modelling have become very complicated [1–3]. In addition, PAs' circuit elements exhibit significant circuit parasitic effects, which are affected by the specifications of wireless signals, such as wide bandwidth and high signal amplitude. Therefore, operating PAs on a wide bandwidth and with high peak-to-average power ratio signals can increase distortion effects in communications [1, 2]. PA behavioural models extensively vary in the aspect of modelling accuracy and computational complexity. A trade-off between modelling accuracy and complexity has become a topic of interest in state-of-the-art model evaluation. In particular, improving the estimation accuracy and reducing the model complexity have become more important in modelling and implementing an efficient digital predistortion. Thus, high accuracy in modelling PAs often results in a better linearisation approach and a lower implementation complexity in digital signal processing.

A model's number of coefficients and mathematical structure are two main consideration aspects for controlling the trade-off between the model accuracy and complexity. For instance, the Taylor model is a simple mathematical function, but it consists of a large number of coefficients and polynomial terms, resulting in a high computational cost. The other empirical models, such as Cann and Rapp models consist of fewer coefficients, but the mathematical functions of these models are more complicated than the Taylor model. The Saleh model is a popular behavioural approach widely used for predicting nonlinear distortion and modelling DPDs in wireless communications [4–11].

A least-squares (LS) method is the commonly used approach for extracting the Saleh parameters. This paper proposes a new approach for estimating the Saleh model using the technical design parameters of solid-state PAs.

Manufacturing datasheets typically provide detailed technical specifications for PAs, such as third-order intercept point (IP_3) and 1-dB compression point (P_{1dB}). An estimation approach of the Saleh amplitude-to-amplitude (AM/AM) model using the parameter IP_3 was proposed in [12]; however, only the third-order intermodulation distortion was considered in the model estimation approach, which exhibits a lower model accuracy. Thus, this paper proposes an accuracy improvement in calculating the Saleh behavioural model by using the PA P_{1dB} parameter in the estimation method. Expressions are derived for calculating the Saleh model's parameters using the design specifications of the PA: gain (G), IP_3, and P_{1dB}. The proposed approach increases the model accuracy and reduces the estimation complexity when compared to the traditional LS method, which typically requires inverting large size matrices. In addition, the LS method requires a large data measurement of input and output signals. A simplified linearisation model is also derived using a two-parameter DPD. The parameters of the DPD model in this work are directly calculated from the PA design specifications. This paper is arranged as follows. Section 1 presents the estimation approach of the PA using the Saleh behavioural model. Section 2 describes the modelling approach of DPD. Section 3 discusses the experimental set-up and modelling results. Finally, conclusions are outlined in Section 4.

2 Saleh model estimation

The memoryless Saleh AM/AM model is an empirical mathematical function as [13]

$$z_S(r) = \frac{\varepsilon r}{1 + \mu r^2} \tag{1}$$

where r and z_S denote the envelopes of the PA input and output signals, respectively. The parameter ε is a small-signal gain, and the parameter μ reflects the adjustment of the saturation and the smoothness in the curvature of the Saleh AM/AM model. The Taylor series of odd-order coefficients is considered in this derivation, which is written as

$$z_T(r) = a_1 r + a_3 r^3 + a_5 r^5 + \cdots \tag{2}$$

where r and z_T are the envelopes of the PA input and output signals respectively, and (a_1, a_3, a_5, …) are the Taylor model coefficients. For simplicity, a fifth-order truncated Taylor model is used in the proposed approach. The same computation procedure can be applied to the Taylor higher nonlinear order. However, the higher-order intermodulation distortions are normally located away from the fundamental frequency in the frequency domain, and they can

be easily filtered out. The coefficients a_1 and a_3 are calculated, respectively, as follows [14, 15]:

$$a_1 = 10^{(G/20)} \tag{3}$$

$$a_3 = \frac{-2}{3}10^{((-2\mathrm{IP}_3+3G)/20)} \tag{4}$$

where G denotes the gain of the PA in dB, the IP_3 is the output third-order intercept point in dBW. The IP_3 is defined as the output power at which the amplitude of the third-order intermodulation harmonic intercepts with the amplitude of the fundamental frequency. The 1-dB compression point is an important measure of the PA nonlinearity, which can specify the dynamic range of the linear region (i.e. back-off region) in the AM/AM conversion. The relationship between the fifth-order Taylor coefficients (a_1, a_3, a_5) and the PA amplitude at the 1-dB compression point $r_{1\mathrm{dB}}$ is given by [16]

$$\frac{5}{8}\left(\frac{a_5}{a_1}\right)r_{1\mathrm{dB}}^4 + \frac{3}{4}\left(\frac{a_3}{a_1}\right)r_{1\mathrm{dB}}^2 + 0.109 = 0 \tag{5}$$

Equation (5) can be expressed as

$$a_5 = \frac{-6a_3}{5r_{1\mathrm{dB}}^2} - \frac{0.174a_1}{r_{1\mathrm{dB}}^4} \tag{6}$$

The $r_{1\mathrm{dB}}^2$ is calculated from the power parameter $P_{1\mathrm{dB}}$ as

$$r_{1\mathrm{dB}}^2 = 2R \times 10^{(P_{1\mathrm{dB}}/10)} \tag{7}$$

where R is the input resistance of the PA and $P_{1\mathrm{dB}}$ is the input power at the 1-dB compression point in dBW. Substituting (7) into (6) for $R = 1$ results in

$$a_5 = \frac{-3}{5}a_3 10^{(-P_{1\mathrm{dB}}/10)} - 0.043a_1 10^{(-P_{1\mathrm{dB}}/5)} \tag{8}$$

Substituting (3) and (4) into (8) results in the following expression of the coefficient a_5 as a function of G, IP_3, and $P_{1\mathrm{dB}}$:

$$a_5 = 0.4 \times 10^{((3G/20)+(-P_{1\mathrm{dB}}/10)+(-IP_3/10))} - 0.043 \times 10^{(G-4P_{1\mathrm{dB}}/20)} \tag{9}$$

PAs operate normally in the AM/AM conversion within the amplitude (0, $r_{1\mathrm{dB}}$) to avoid high nonlinear effects and signal to clip in the saturation region. Thus, the minimum squared errors between the Saleh model and fifth-order Taylor model in the back-off region is described as

$$\begin{cases} \underset{(a_1\ \ a_3\ \ a_5)}{\text{minimising}} & ((z_T(r) - z_S(r))^2) \\ \text{subject to} & (0 \le r \le r_{1dB}) \end{cases} \tag{10}$$

The variable r denotes the amplitude of the input signal, which is specified from zero to the amplitude near the 1-dB compression point as (0, $1/\sqrt{8\mu}$) [12]. Therefore, the squared errors function $e^2(r)$ is

$$e^2(r) = \left(a_1 r + a_3 r^3 + a_5 r^5 - \frac{\varepsilon r}{1+\mu r^2}\right)^2_{r\in(0,1/\sqrt{8\mu})} \tag{11}$$

The sum of squared errors (SSE) represents the integral over the defined amplitude range in (10). This can be written as

$$e_T^2 = \int_0^{1/\sqrt{8\mu}} \left(a_1 r + a_3 r^3 + a_5 r^5 - \frac{\varepsilon r}{1+\mu r^2}\right)^2 \mathrm{d}r \tag{12}$$

where e_T^2 is the SSE. The integral computation of (12) is (see (13)) . The minimum SSE is calculated such that the gradient of (13) approaches zero

$$\mathrm{Min}(e_T^2) \Rightarrow \nabla(e_T^2) = 0 \tag{14}$$

$$\nabla(e_T^2) = \left(\frac{\partial e_T^2}{\partial a_1}, \frac{\partial e_T^2}{\partial a_3}, \frac{\partial e_T^2}{\partial a_5}\right) = (0,0,0) \tag{15}$$

The following equations are obtained by substituting (13) into (15) and calculating the gradient:

$$\begin{aligned} &\big(630\sqrt{2}a_5 + 6160\sqrt{2}a_3\mu + 63,360\sqrt{2}a_1\mu^2 \\ &\quad -218,330,112\sqrt{2}\varepsilon\mu^2 + 908,328,960\varepsilon\mu^2\tan^{-1}(1/2\sqrt{2})\big) \\ &\quad /\big(454,164,480\mu^5\sqrt{\mu}\big) = 0 \end{aligned} \tag{16}$$

$$\begin{aligned} &\big(63,360\sqrt{2}a_5\mu^2 + 709,632\sqrt{2}a_3\mu^3 + 9,461,760\sqrt{2}a_1\mu^4 \\ &\quad -22,7082,240\sqrt{2}\varepsilon\mu^4 + 908,328,960\varepsilon\mu^4\tan^{-1}(1/2\sqrt{2})\big) \\ &\quad /\big(454,164,480\mu^5\sqrt{\mu}\big) = 0 \end{aligned} \tag{17}$$

$$\begin{aligned} &\big(6160\sqrt{2}a_5\mu + 63,360\sqrt{2}a_3\mu^2 + 709,632\sqrt{2}a_1\mu^3 \\ &\quad +217,620,480\sqrt{2}\varepsilon\mu^3 - 908,328,960\varepsilon\mu^3\tan^{-1}(1/2\sqrt{2})\big) \\ &\quad /\big(454,164,480\mu^5\sqrt{\mu}\big) = 0 \end{aligned} \tag{18}$$

The Taylor coefficients (a_1, a_3, a_5), in terms of the Saleh parameters ε and μ, are calculated by solving (16)–(18) for a_1, a_3, and a_5 as follows:

$$a_1 = 93,093\varepsilon - 193698.75\varepsilon\sqrt{2}\tan^{-1}(1/2\sqrt{2}) \simeq 0.99\varepsilon \tag{19}$$

$$\begin{aligned} a_3 = &-3,432,912\varepsilon\mu \\ &+7,142,940\sqrt{2}\varepsilon\mu\tan^{-1}(1/2\sqrt{2}) \simeq -0.99\varepsilon\mu \end{aligned} \tag{20}$$

$$\begin{aligned} a_5 = &24550310.4\varepsilon\mu^2 \\ &-51,082,416\sqrt{2}\varepsilon\mu^2\tan^{-1}(1/2\sqrt{2}) \simeq 0.82\varepsilon\mu^2 \end{aligned} \tag{21}$$

Equations (19)–(21) are nonlinear in terms of ε and μ. Thus, logarithmic functions are applied on (19)–(21) for linear transformation and re-formulating the equations in a matrix form as

$$\begin{bmatrix} 1 & 0 \\ 1 & 1 \\ 1 & 2 \end{bmatrix} \begin{bmatrix} \log(\varepsilon) \\ \\ \log(\mu) \end{bmatrix} = \begin{bmatrix} \log(1.01a_1) \\ \log(-1.01a_3) \\ \log(1.21a_5) \end{bmatrix} \tag{22}$$

Equation (22) represents a logarithmic transformation between the Saleh parameters and fifth-order Taylor coefficients. Substituting (3), (4), and (9) into (22), results in a matrix equation as

$$\begin{aligned} e_T^2 = \big\{&\big(315\sqrt{2}a_5^2 + 6160\sqrt{2}a_3a_5\mu + 31680\sqrt{2}(a_3^2 + 2a_1a_5)\mu^2 \\ &-227082240\sqrt{2}\mu^2(a_5 + \mu(a_1\mu - a_3))\varepsilon - 50462720\sqrt{2}\mu^4\varepsilon^2 \\ &+709632\sqrt{2}\mu^2(a_1a_3\mu - a_5\varepsilon) + 4730880\sqrt{2}\mu^2(a_1^2\mu^2 + 2(a_5 - a_3\mu)\varepsilon\big) \\ &+227082240\mu^2\varepsilon(4a_5 + \mu(-4a_3 + \mu(4a_1 + \varepsilon))) \\ &\tan^{-1}(1/2\sqrt{2})\big)/(454164480\mu^{(11/2)})\big\} \end{aligned} \tag{13}$$

$$\begin{bmatrix} 1 & 0 \\ 1 & 1 \\ 1 & 2 \end{bmatrix} \begin{bmatrix} \log(\varepsilon) \\ \log(\mu) \end{bmatrix} = \begin{bmatrix} \dfrac{G}{20} + 0.004 \\ \dfrac{-\mathrm{IP}_3}{10} + \dfrac{3G}{20} - 0.17 \\ \log[0.48 \times 10^{((3G/20)+(-IP_3/10)+(-P_{1\,\mathrm{dB}}/10))} \\ -0.048 \times 10^{((G/20)+(-P_{1\,\mathrm{dB}}/5))}] \end{bmatrix} \tag{23}$$

The matrix notation of (23) is

$$\boldsymbol{K} \cdot \boldsymbol{S} = \boldsymbol{C} \tag{24}$$

The (2×1) column vector $\boldsymbol{S}$ is a logarithmic operation of the Saleh coefficients, the (3×1) column vector $\boldsymbol{C}$ includes the parameters of the PA: G, IP_3, and $P_{1\mathrm{dB}}$. $\boldsymbol{K}$ is a (3×2) matrix consisting of constants. Using linear algebra on (24) to separate the matrices in the sense of the LS, results in

$$\boldsymbol{S} = (\boldsymbol{K}^T\boldsymbol{K})^{-1}\boldsymbol{K}^T\boldsymbol{C} \tag{25}$$

The pseudo-inverse of $\boldsymbol{K}$ can be easily calculated
(see (26))
(see (27))
Finally, the Saleh coefficients in (27) are calculated by simplifying the matrices' computation in (26).

3 DPD model

DPD models are popular linearisation techniques in wireless communications. DPD models are implemented with high accuracy in the digital signal domain prior to baseband up-conversion, as illustrated in Fig. 1. DPD models perform typical gain expansion in AM/AM conversion to compensate for the gain compression characteristics in RF PAs. The modelling of a DPD involves basically calculating the mathematical inverse function of the PA's behavioural model [17–19]. Thus, the inverse function of the Saleh model is depicted in (28), which is calculated by solving a quadratic equation of the Saleh model.

$$D[h] = \frac{\varepsilon - \sqrt{\varepsilon^2 - 4\mu h^2}}{2\mu h} \tag{28}$$

where $D[.]$ is the AM/AM model of the DPD, h is the DPD input signal. ε and μ are the coefficients of the Saleh model. The DPD output in (28) is real; therefore, the dynamic amplitude range of the input signal is

$$0 < h < \sqrt{\frac{\varepsilon^2}{4\mu}} \tag{29}$$

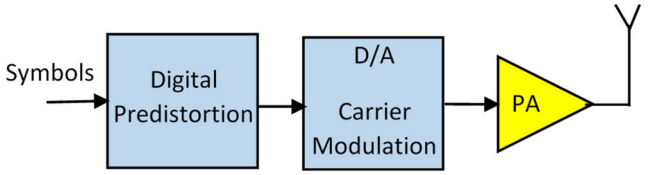

Fig. 1 *Simplified block diagram of a wireless transmitter using DPD*

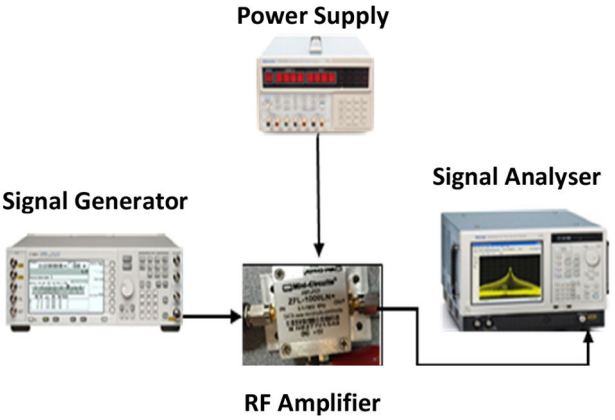

Fig. 2 *Experimental architecture for model evaluation*

Finally, the proposed DPD model in (30) is calculated by substituting the Saleh parameters from (27) into (28). The presented DPD model in (30) based on the parameters of the PA can achieve a lower estimation complexity and computational cost, as compared to the mathematical inversion of the fifth-order Taylor model (see (30)) .

The dynamic range of the proposed DPD input amplitude is calculated by substituting the Saleh parameters from (27) into (29) and simplifying the expression to obtain (see (31)) .

4 Experimental results

The experimental set-up for PA modelling and validation is shown in Fig. 2. The measurement data was obtained using a GaAs PA ZFL-1000LN from Mini-Circuit. The PA was excited by a two-tone signal at a 900 MHz frequency with 50 kHz tone-spacing. The two-tone signal was generated from a Keysight E4438C signal generator. The output of the PA was acquired by a Tektronix RSA 6120A spectrum analyser.

Fig. 3 illustrates the PA intermodulation distortion using the two-tone test. This test was used to calculate the IP_3 of the PA [14, 15]. The measured parameters of the PA are $G = 22.45$ dB, $\mathrm{IP}_3 = 12.81$ dBm, and output $P_{1\,\mathrm{dB}} = 2.25$ dBm. Fig. 4 shows the results

$$\begin{bmatrix} \log(\varepsilon) \\ \log(\mu) \end{bmatrix} = \begin{bmatrix} 5/6 & -1/2 \\ 1/3 & 0 \\ -1/6 & 1/2 \end{bmatrix}^T \begin{bmatrix} \dfrac{G}{20} + 0.004 \\ \dfrac{-IP_3}{10} + \dfrac{3G}{20} - 0.17 \\ \log\left[0.48 \times 10^{((3G/20)+(-IP_3/10)+(-P_{1\,\mathrm{dB}}/10))}\right. \\ \left. -0.048 \times 10^{((G/20)+(-P_{1\,\mathrm{dB}}/5))}\right] \end{bmatrix} \tag{26}$$

$$\begin{bmatrix} \varepsilon \\ \mu \end{bmatrix} = \begin{bmatrix} 10^{((11G/120)+(-4/75)/(-IP_3/30))}\left(0.48 \times 10^{((3G/20)+(-IP_3/10)+(-P_{1\,\mathrm{dB}}/10))} - 0.048 \times 10^{((G/20)+(-P_{1\,\mathrm{dB}}/5))}\right)^{-1/6} \\ 10^{-(G+0.008/40)}\left(0.48 \times 10^{((3G/20)+(-IP_3/10)+(-P_{1\,\mathrm{dB}}/10))} - 0.048 \times 10^{((G/20)+(-P_{1\,\mathrm{dB}}/5))}\right)^{1/2} \end{bmatrix} \tag{27}$$

$$D[h] = \frac{1 - \sqrt{1 - 4h^2 \times 10^{((-5G/24)+(\mathrm{IP}_3/15)+(157/1500))}\left(0.48 \times 10^{((3G/20)+(-\mathrm{IP}_3/10)+(-P_{1\,\mathrm{dB}}/10))} - 0.048 \times 10^{((G/20)+(-P_{1\,\mathrm{dB}}/5))}\right)^{5/6}}}{2h \times 10^{((-7G/60)+(\mathrm{IP}_3/30)+(4/75))}\left(0.48 \times 10^{((3G/20)+(-\mathrm{IP}_3/10)+(-P_{1\,\mathrm{dB}}/10))} - 0.048 \times 10^{((G/20)+(-P_{1\,\mathrm{dB}}/5))}\right)^{2/3}} \tag{30}$$

$$0 < h < \frac{1}{2}\frac{10^{((5G/48)+(-\mathrm{IP}_3/30)+(-157/3000))}}{\left(0.48\times 10^{((3G/20)+(-\mathrm{IP}_3/10)+(-P_{1\,\mathrm{dB}}/10))}-0.048\times 10^{((G/20)+(-P_{1\,\mathrm{dB}}/5))}\right)^{5/12}} \tag{31}$$

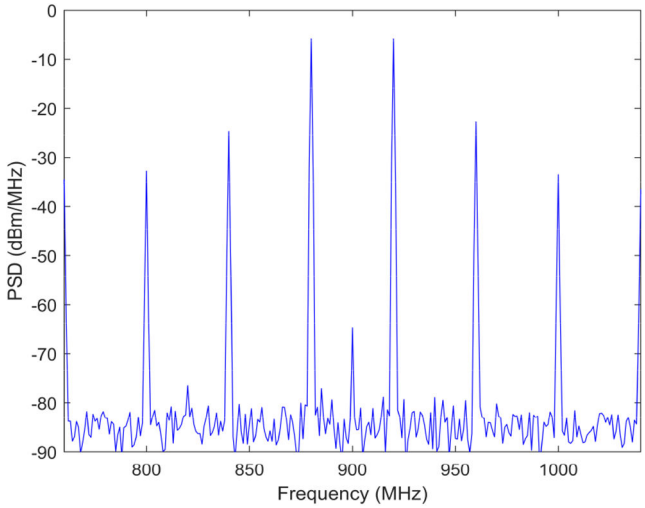

Fig. 3 *Two-tone intermodulation distortion for the PA*

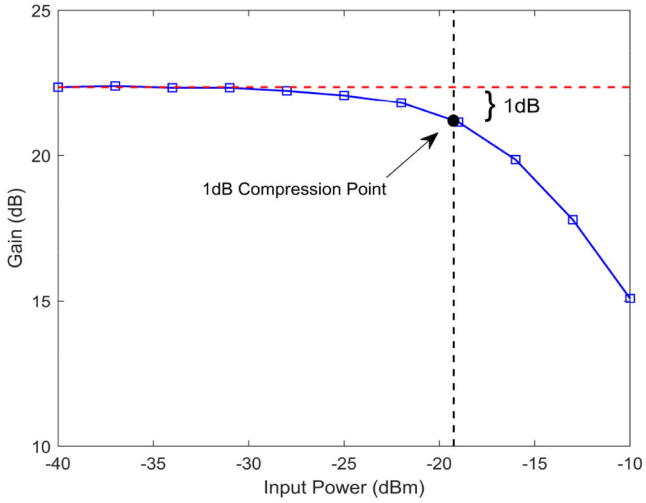

Fig. 4 *Measured gain compression curve for calculating the 1-dB compression point*

of the measured gain and 1-dB compression point for the PA as obtained by sweeping the amplitude of the two-tone test.

The amplitude conversion in the PA input and output of the two-tone signal is illustrated in Fig. 5, as obtained from a two-tone experiment. The estimated models of both the fifth-order Taylor and Saleh models using the presented approach are also overlaid on the same figure. This shows that the AM/AM conversions of the Saleh model and fifth-order Taylor model match well with the measurement results. The normalised mean-square error (NMSE) and adjacent channel error power ratio (ACEPR) [20] were both used for the PA model validation. The NMSE between the measured and modelled output signals was calculated using

$$\eta = 10\times\log_{10}\left(\frac{\sum_n |z_{\mathrm{meas}}(n)-z_{\mathrm{mod}}(n)|^2}{\sum_n |z_{\mathrm{meas}}(n)|^2}\right) \tag{32}$$

where η is NMSE in dB, $z_{\mathrm{meas}}(n)$ and $z_{\mathrm{mod}}(n)$ are the measured and modelled signals of the PA. The ACEPR is the model evaluation in the frequency domain, which can be expressed as

$$\mathrm{ACEPR} = 10\times\log_{10}\left(\frac{\int_{f_{\mathrm{adj}}}|Z_{\mathrm{meas}}(f)-Z_{\mathrm{mod}}(f)|^2\mathrm{d}f}{\int_{f_{\mathrm{chan}}}|Z_{\mathrm{meas}}(f)|^2\mathrm{d}f}\right) \tag{33}$$

where $Z_{\mathrm{meas}}(f)$ and $Z_{\mathrm{mod}}(f)$ are the Fourier transform of the measured and modelled signals, respectively. f_{adj} and f_{chan} are the frequency bands of the adjacent channels and carrier channel, respectively. Table 1 illustrates the model accuracy evaluation in both the NMSE and ACEPR.

The DPD model is typically evaluated in a frequency domain using the adjacent channel power ratio (ACPR), which is defined as

$$\mathrm{ACPR} = 10\times\log_{10}\left(\frac{\int_{f_{\mathrm{adj}}}|Z(f)|^2\mathrm{d}f}{\int_{f_{\mathrm{chan}}}|Z(f)|^2\mathrm{d}f}\right) \tag{34}$$

where $Z(f)$ is the Fourier transform of the PA baseband output signal. The effects of the parameters IP_3 and $P_{1\mathrm{dB}}$ on the Saleh parameters in (27) are illustrated in Fig. 6 and Fig. 7. The surface plot in Fig. 6 shows a steady slope and increasing rate of the Saleh parameter ε with respect to both IP_3 and $P_{1\mathrm{dB}}$. The Saleh parameter μ is very sensitive to the variation of both IP_3 and $P_{1\mathrm{dB}}$, as shown in Fig. 7, which illustrates a sharply increasing rate of the computed surface versus the swept parameters IP_3 and $P_{1\mathrm{dB}}$. This

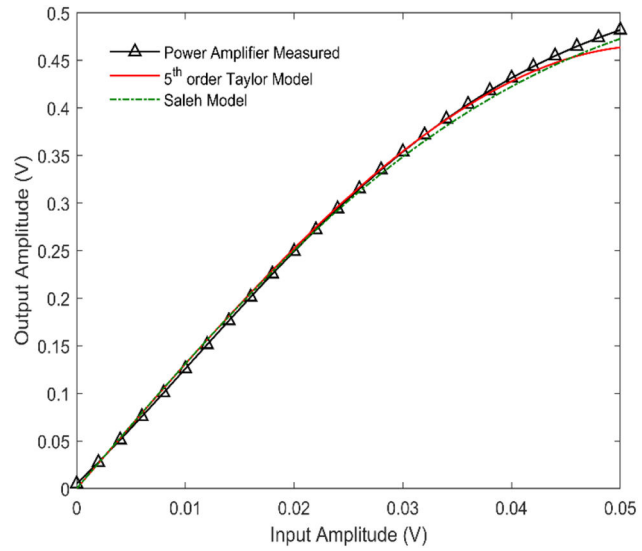

Fig. 5 *Measured and modelled amplitude-to-amplitude results of the PA*

Table 1 Accuracy evaluation in NMSE and ACEPR for the Saleh estimation approaches

Estimation approach	Model parameters	NMSE, dB	ACEPR, dB
scenario (1)	G, IP_3	−34.32	−42.52
scenario (2)	G, IP_3, $P_{1\,\mathrm{dB}}$	−35.85	−43.31

is because the Saleh parameter μ normally adjusts the model's nonlinear characteristics.

The estimation accuracy using this approach is illustrated in Fig. 8 using the residual errors between the PA measured and modelled amplitude in time domain. In addition, the model evaluation in frequency domain using the power spectral density of WCDMA signal is shown in Fig. 9.

The DPD model used in the proposed approach was calculated in MATLAB and evaluated using the same experiment based on the WCDMA signal. Fig. 10 shows the output power spectral density of the PA using two scenarios: PA without predistortion, which shows spectrum regrowth due to the nonlinear intermodulation distortion, and PA with predistortion, which shows a spectrum improvement in the adjacent channels. Table 2

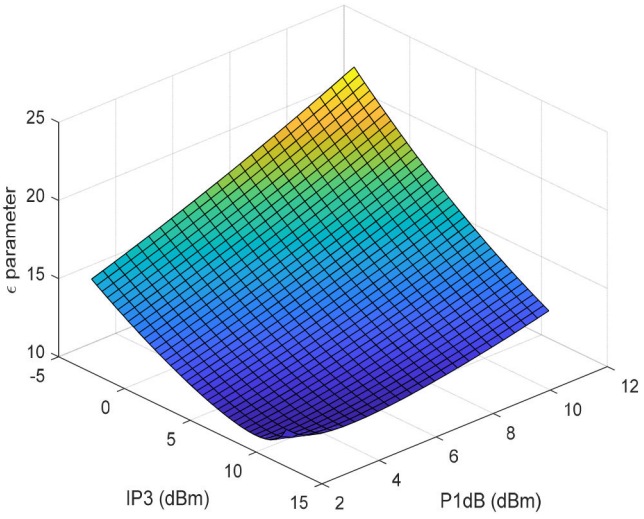

Fig. 6 *Computed the Saleh parameter ε versus the third-order intercept point and 1-dB compression point*

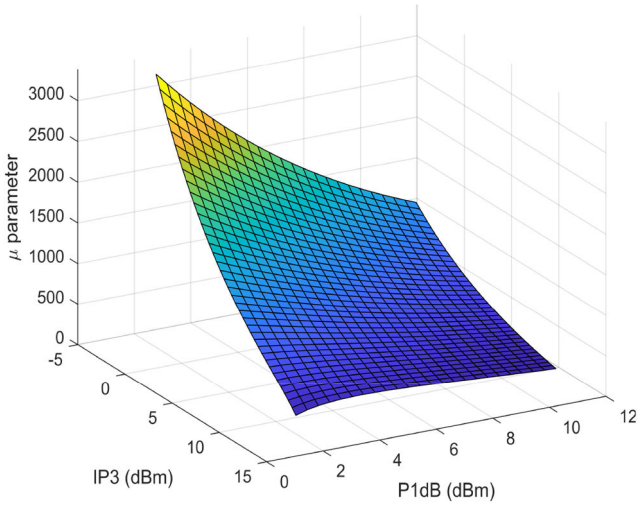

Fig. 7 *Computed the Saleh parameter μ versus the third-order intercept point and 1-dB compression point*

Table 2 ACPR evaluation results for the PA

WCDMA signal	Without linearisation, dBc	With linearisation, dBc
upper band	−18.42	−31.23
lower band	−19.59	−32.12

illustrates the calculated ACPR for evaluating the linearisation approach in the upper and lower adjacent channels.

5 Conclusions

An approach for estimating the coefficients of the Saleh model was presented in this paper. The calculated expressions define new relationships between the parameters of the Saleh model and the technical design parameters of RF PAs: gain, third-order intercept point, and 1-dB compression point. The fifth-order Taylor model was employed in this derivation to estimate the Saleh model by minimising the objective squared error function between the two behavioural models.

The accuracy of the proposed modelling approach was evaluated using the NMSE and ACEPR figures-of-merit, between the measured and modelled signals. An estimation approach of a low-complexity DPD was also calculated in this paper as a function of the PA's parameters. The DPD model was evaluated in the frequency domain using ACPR. The DPD model achieved a 12.81/12.59 dBc improvement in the ACPR of the WCDMA signal.

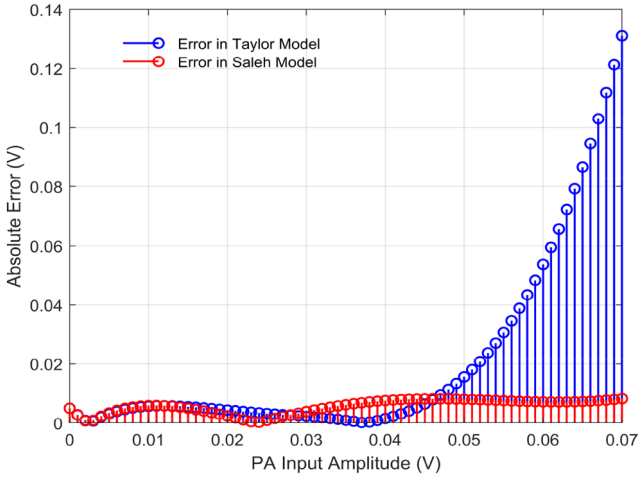

Fig. 8 *Absolute residual errors of the Saleh model and fifth-order Taylor model, both with respect to the PA measured amplitude*

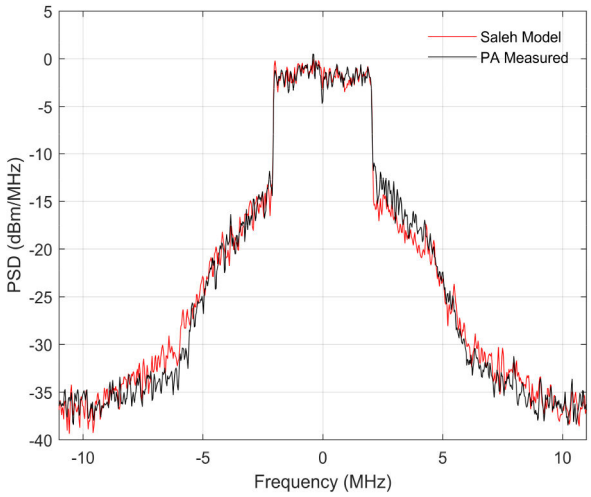

Fig. 9 *Measured and modelled output spectrum of the WCDMA signal for the PA*

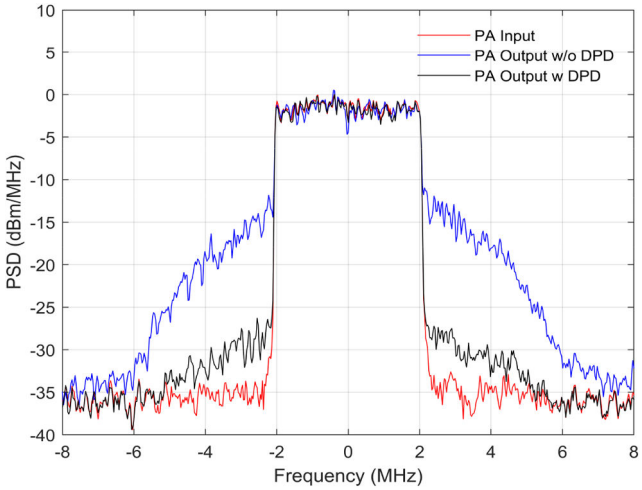

Fig. 10 *Power spectrum density for the PA, before and after DPD*

6 Acknowledgments

The authors acknowledge Prof. Jeffrey S. Ovall from the Fariborz Maseeh Department of Mathematics and Statistics at Portland State University for his suggestion regarding the mathematical derivations. Publication of this article in the *Journal of Engineering* was funded by Portland State University's open access fund.

7 References

[1] Ghannouchi, F., Hammi, O., Helaoui, M.: '*Behavioral modeling and predistortion of wideband wireless transmitters*' (John Wiley, Hoboken, NJ, USA, 2015, 1st edn.)

[2] Schreurs, D., O'Droma, M., Goacher, A.A*., et al.*: '*RF power amplifier behavioral modeling*' (Cambridge University Press, Cambridge, UK, 2008, 1st edn.)

[3] Cann, A.J.: 'Improved nonlinearity model with variable knee sharpness', *IEEE Trans. Aerosp. Electron. Syst.*, 2012, **48**, (4), pp. 3637–3646

[4] Al-kanan, H., Li, F., Tafuri, F.: 'Extended Saleh model for behavioral modeling of envelope tracking power amplifiers'. IEEE 18th Wireless and Microwave Technology Conf. (WAMICON), Cocoa Beach, FL, USA, 2017, pp. 1–4

[5] Al-kanan, H., Tafuri, F., Li, F.: 'Hysteresis nonlinearity modeling and linearization approach for envelope tracking power amplifiers in wireless systems', *Microelectron. J.*, 2018, **82**, pp. 101–107

[6] Ping-hui, L., Peng, W.: 'Wiener-Saleh modeling of nonlinear RF power amplifiers considering memory effects'. 2010 Int. Conf. on Microwave and Millimeter Wave Technology, Chengdu, China, 2010, pp. 1447–1449

[7] O'Droma, M., Meza, S., Lei, Y.: 'New modified Saleh models for memoryless nonlinear power amplifier behavioural modelling', *IEEE Commun. Lett.*, 2009, **13**, (6), pp. 399–401

[8] Ren, Z., Chen, H., Chen, W.: 'Distortion-characteristic estimation predistorter for high efficiency power amplifiers', *IET Sig. Process.*, 2016, **10**, (9), pp. 1024–1030

[9] Yoda, D., Ochiai, H.: 'Decision region optimization and metric-based compensation of memoryless nonlinearity for APSK systems', *IEEE Trans. Broadcast.*, 2018, **64**, (2), pp. 281–292

[10] Gülgün, Z., Yilmaz, A.Ö.: 'Detection schemes for high order M-ary QAM under transmit nonlinearities', *IEEE Trans. Commun.*, 2019, **67**, (7), pp. 4825–4834

[11] Ochiai, H.: 'An analysis of band-limited communication systems from amplifier efficiency and distortion perspective', *IEEE Trans. Commun.*, 2013, **61**, (4), pp. 1460–1472

[12] Al-kanan, H., Yang, X., Li, F.: 'Saleh model and digital predistortion for power amplifiers in wireless communications using the third-order intercept point', *J. Electron. Test., Theory Appl.*, 2019, **35**, (3), pp. 359–365

[13] Saleh, A.: 'Frequency independent and frequency dependent nonlinear model of TWT amplifiers', *IEEE Trans. Commun.*, 1981, **COM-29**, pp. 1715–1720

[14] Li, X., Liu, C., Xu, Y*., et al.*: 'Obtaining polynomial coefficients from intercept points of RF power amplifiers', *Electron. Lett.*, 2012, **48**, (19), pp. 1238–1240

[15] Li, X., Li, F.: 'RF power amplifier's nonlinear modelling with memory effect', *Int. J. Electron. Lett.*, 2013, **1**, (1), pp. 44–49

[16] Cho, C., Eisenstadt, W., Stengel, B*., et al.*: 'IIP3 estimation from the gain compression curve', *IEEE Trans. Microw. Theory Tech.*, 2005, **53**, (4), pp. 1197–1202

[17] Marsalek, R., Jardin, P., Baudoin, G.: 'From post-distortion to pre-distortion for power amplifiers linearization', *IEEE Commun. Lett.*, 2003, **7**, (7), pp. 308–310

[18] Nguyen, T.M., Yoh, J., Lee, C.H*., et al.*: 'Modeling of HPA and HPA linearization through a predistorter: global broadcasting service applications', *IEEE Trans. Broadcast.*, 2003, **49**, (2), pp. 132–141

[19] Jang, K., Ryu, H., Ryu, S*., et al.*: 'Spectrum characteristics and predistortion gain in the nonlinear high power amplifier (HPA)'. 2017 Int. Conf. on Information and Communication Technology Convergence (ICTC), Jeju, South Korea, 2017, pp. 931–934

[20] IsaksSon, M., Wisell, D., Ronnow, D.: 'A comparative analysis of behavioral models for RF power amplifiers', *IEEE Trans. Microw. Theory Tech.*, 2006, **54**, (1), pp. 348–359